Agarose-collagen I hydrogels: impact of the matrix stiffness on the growth of breast cancer cell lines spheroids and on drug penetration

ALESSANDRA QUARTA[1], Nunzia Gallo[2], Daniele Vergara[3], Luca Salvatore[2], Concetta Nobile[4], Andrea Ragusa[3], and Antonio Gaballo[4]

[1]CNR
[2]Università del Salento
[3]Universita del Salento
[4]Consiglio Nazionale delle Ricerche

March 7, 2021

Abstract

Three-dimensional (3D) cell culture systems mimic the structural complexity of the tissue microenvironment that includes the extracellular matrix (ECM) in addition to the cellular components Thus, 3D culture systems are increasingly important as they resemble the ECM-cell and cell-cell physical interactions occurring in vivo. So far, several scaffold-based culture systems and techniques have been proposed as valuable approaches for large-scale production of spheroids, but often suffering of poor reproducible conditions or high costs of production. In this work we present a reliable 3D culture system based on collagen I-blended agarose hydrogels and show how the variation of the agarose weight percentage affects the physical and mechanical properties of the resulting hydrogel, being that with a lower amount of agarose more permeable, softer and more prone to degradation compared to hydrogels with higher agarose concentrations. We have also evaluated the effect of the different physical and mechanical properties of the agarose hydrogels on the growth, size, morphology and cell motility of spheroids obtained by culturing three different breast cancer cell lines (MCF-7, MDA-MB-361and MDA-MB-231). As proof of concept, the cisplatin penetration and its cytotoxic effect on the tumor spheroids was evaluated as function of the hydrogel stiffness. Noteworthy, the possibility to recover the spheroids from the hydrogels for further processing and other biological studies has been also considered.

Article

Agarose-collagen I hydrogels: impact of the matrix stiffness on the growth of breast cancer cell lines spheroids and on drug penetration

Alessandra Quarta[1,*], Nunzia Gallo[2], Daniele Vergara[3], Luca Salvatore[2], Concetta Nobile[1], Andrea Ragusa[1,3] and Antonio Gaballo [1,*]

[1] CNR Nanotec, Institute of Nanotechnology, via Monteroni, 73100 Lecce, Italy[2] Department of Engineering for Innovation, University of Salento, via Monteroni, 73100 Lecce, Italy[3] Department of Biological and Environmental Sciences and Technologies, University of Salento, via Monteroni, 73100 Lecce, Italy* Correspondence: alessandra.quarta@nanotec.cnr.it (A.Q.); antonio.gaballo@nanotec.cnr.it (A.G.)**Keywords:** spheroids; hydrogel; collagen; mammary spheroids

Abstract:

Three-dimensional (3D) cell culture systems mimic the structural complexity of the tissue microenvironment that includes the extracellular matrix (ECM) in addition to the cellular components Thus, 3D culture systems are increasingly important as they resemble the ECM-cell and cell-cell physical interactions occurring *in vivo*

. So far, several scaffold-based culture systems and techniques have been proposed as valuable approaches for large-scale production of spheroids, but often suffering of poor reproducible conditions or high costs of production. In this work we present a reliable 3D culture system based on collagen I-blended agarose hydrogels and show how the variation of the agarose weight percentage affects the physical and mechanical properties of the resulting hydrogel, being that with a lower amount of agarose more permeable, softer and more prone to degradation compared to hydrogels with higher agarose concentrations. We have also evaluated the effect of the different physical and mechanical properties of the agarose hydrogels on the growth, size, morphology and cell motility of spheroids obtained by culturing three different breast cancer cell lines (MCF-7, MDA-MB-361and MDA-MB-231). As proof of concept, the cisplatin penetration and its cytotoxic effect on the tumor spheroids was evaluated as function of the hydrogel stiffness. Noteworthy, the possibility to recover the spheroids from the hydrogels for further processing and other biological studies has been also considered.

1. Introduction

Three-dimensional cell culture models such as multicellular spheroids and organoids have been demonstrated to mimic several biological processes *in vitro* much better than monolayer cell cultures (Cui, Hartanto, & Zhang, 2017). There are essentially two methods to produce uniform-size multicellular spheroids: scaffold free, in which the cells are prevented from adhering to substrates but not to each other thus forming spheroids, and scaffold- or matrix-based, in which cells are embedded into a three-dimensional (3D) biomaterial such as a hydrogel. The latter, usually composed of polymers, has the advantage to provide a physical structure comparable, in terms of stiffness and viscoelasticity, to the extracellular matrix (ECM) *in vivo* and it is thus able to reproduce not only cell-cell interactions, but also cell-matrix interplays directly related to phenomena associated with cell growth (cell fate) such as cytoskeletal organization, gene expression, nutrients diffusion, pH and hypoxia (Singh, Brito, & Lammerding, 2018). This makes matrix-based spheroids increasingly important for studying solid tumors microenvironment and the response to drug treatments (Nath & Devi, 2016).

Among several 3D biomaterials, hydrogels of complex biological origin have been used in many studies. The most common are Matrigel^{TM}, derived from Engelbreth-Holm-Swarm mouse tumor sarcoma, and other basement membrane-rich matrices. These hydrogels contain matrix membrane proteins, hormones and soluble growth factors whose composition may vary among different batches. This aspect limits their use because, although they allow for the growth in three dimensions, the batch-to-batch variability could potentially alter cell culture systems and experimental results. Thus, other simple hydrogels, without hormones and growth factors, able to maximize reproducibility and offering the possibility to tune biochemical as well as mechanical properties, have been considered to grow spheroids. Hydrogels with these features are made of natural, synthetic or hybrid materials, such as alginate, agarose, collagen, hyaluronic acid and polyethylene glycol (Cui et al., 2017; Teruki, Kimiko, & Yasuhiko, 2020).

Among them, agarose is an inert, inexpensive, and easily available polysaccharide derived from red marine algae and consisting of repeated units of b-1,3-linked-D-galactose and a-1,4-linked 3,6-anhydro-L-galactose. It possesses excellent biocompatibility, optimal gelling features and tunable mechanical properties that boosted its use as biomaterial for the manufacturing of tissue engineering scaffolds (Anderson & Johnstone, 2017; López-Marcial et al., 2018). In addition, thanks to the ease of preparation, it has been recently exploited as non-adhesive and micromolded substrate for the growth of tumor spheroids based on multicellular aggregation (Napolitano et al., 2007; Tang, Liu, & Chen, 2016). Nevertheless, due to its poor bioadhesivity, as it lacks cell adhesion motifs, its use as ECM-mimicking material is very limited.

On the other hand, type I collagen is the main protein component of the ECM in mammals. The presence of cellular binding sites (i.e. the "GxOGER" sequence, where "R" is arginine, "G" is glycine, "D" in aspartate, "O" is hydroxyproline, "E" is glutamate and "x" is a hydrophobic amino acid) that promote cell adhesion and proliferation, and regulate cell signaling pathways, makes collagen highly bioactive and suitable for the development of natural material-based hydrogels for cell culture studies (Davidenko et al., 2018; Davidenko et al., 2016; Hamaia & Farndale, 2014; Tibbitt & Anseth, 2009). In addition, it plays a crucial role in tumor

progression and invasion (Li & Kumacheva, 2018). It can form hydrogels through self-aggregation of the fibers or by physical and chemical crosslinking, but is suffers of poor mechanical properties, limited stability over time and high costs (Caliari & Burdick, 2016).

In this sense, blended hydrogels composed of agarose and collagen combine the mechanical properties of agarose and the biomimetic nature of collagen (Ulrich, Jain, Tanner, MacKay, & Kumar, 2010). As far as we know, only one study described the use of hydrogels containing agarose and collagen as matrices for the formation of tumor spheroids. In detail, composite hydrogels made of alginate, marine collagen, and agarose were prepared and the growth and viability of spheroids derived from ovarian cancer and lymphoma cell lines were monitored up to 14 days (Shin et al., 2016). Notably, twoother studies described the use of agarose-collagen blend hydrogels that were not used to promote the growth of spheroids, but to unravel the effects of biophysical cues on cellular mechanobiology of 2D intervertebral disc cells(Cambria et al., 2020) and glioblastoma spheroids that had been previously prepared by the hanging drop method and then loaded into the hydrogel (Ulrich et al., 2010). Both works evidence the crucial role of the hydrogel stiffness and adhesivity as driving forces that modulate the cell plasticity and connect the biological functionality to the surrounding physical stimuli. Thus, the interplay between the hydrogel and the cells embedded within it depends on what the cells sense and how they reply to the host environment. In living tissues, the stiffness spans from few tens Pa in intestinal mucus to GPa of bones, and variations of the mechanical properties are typically associated to diseases and cancer development (Guimarães, Gasperini, Marques, & Reis, 2020). In the case of breast, it has been shown that the stiffness increases from hundreds Pa to few kPa when the normal tissue undergoes to tumor transformation, due to the remodeling of the ECM (Butcher, Alliston, & Weaver, 2009).

Therefore, artificial matrices resembling the physical properties of the naïve tumor environment may facilitate the study of 3D tumors behavior in vitro and predict their response to modifications of the mechanical cues or to drug treatments, as it occurs during cancer progression and metastatization (Singh et al., 2018).

In this work we have developed agarose-collagen blended hydrogels with variable agarose amount (from 0.5 to 0.125%) and analyzed the growth of breast tumor spheroids of three different breast cancer cell lines: the luminal estrogen receptor positive cells, MCF-7 and MDA-MB-361, and the triple negative model, MDA-MB-231, for comparative analysis.

The preparation method is simple, quick and highly reproducible. By embedding individual cells into the liquid mixture of agarose and collagen, prior to the gelation, allows to follow up the growth of the 3D tumoroids over time. The physical properties of the matrices have been thoroughly investigated and the characteristics of the spheroids' growth were related to the hydrogel features. Upon variation of the agarose percentage, the physical and mechanical properties of the matrices can be tuned, and in turn, the growth kinetic and the morphology of the spheroids also vary, confirming their sensitivity to the environment stiffness. Noteworthy, the optical transparency of agarose facilitates the daily analysis of spheroids that result more compact in stiffer hydrogels, while they look loosened with cellular protrusions and disseminated cells in softest matrices. Remarkably, tumor spheroids can be recovered upon enzymatic treatment of the hydrogels with agarase, with a yield of 100% in the case of the matrices containing the lower amount of agarose (equal to 0.125%). Preliminary drug testing studies with cisplatin evidenced a cytotoxic response that depends on the agarose percentage concentration. Overall, the results show that agarose-collagen blended hydrogels are suitable modular matrices for tumor spheroids culturing and for evaluating drug protocols efficacy.

2. Materials and Methods

The following chemicals were obtained from commercial sources and used as received. Soluble type I collagen from calf skin was purchased from Symatese (Chaponost, France). Agarose, β-Agarase from Pseudomonas atlantica, FITC-labelled Hyaluronic acid, Transferrin-TRITC, Dulbecco's Modified Eagle Medium high glucose (DMEM), fetal bovine serum (FBS), penicillin and streptomycin were purchased from Sigma–Aldrich, Italy. Live-Dead assay and MitoTracker Red CMXRos were purchased from Thermo Fisher. Ultrapure grade water with a conductivity of 18.2 M cm was used in all experiments.

2.1. Preparation of the hydrogels

Agarose was dissolved in sterile PBS to obtain a 1% (w/v) solution by heating on a hot plate. The aqueous suspension of 0.1% (w/v) type I collagen was obtained by slowly hydrating collagen flakes in distilled water for 3 h, under magnetic stirring at 4 °C.

To prepare the agarose-collagen blended hydrogels (A-C), the warm agarose solution (at around 45 °C, the gel point is at 36 °C) was added to the collagen suspension. The hydrogels were prepared inside the wells of a 24 well plate: each well was loaded with 1 mL of A-C hydrogel. The starting agarose solution was diluted to obtain 3 different working concentrations, 0.5, 0.25, and 0.125%, respectively. The starting collagen solution was diluted to 0.02% in the final blend. The components were mixed gently with a glass rod and allowed to gel at room temperature. The gelation time varied from 30 seconds up to 10 minutes in the case of hydrogels containing 0.5% and 0.125% agarose, respectively. All the glassware was sterilized in an autoclave prior to be used, and the preparation of the hydrogels was carried out under a laminar flow hood. The preparation scheme is presented in Figure 1.

2.2. Characterization of the hydrogels

Hydrogels Scanning Electron Microscopy (SEM). Surface morphology and porosity of the hydrogels were investigated using SEM imaging techniques. SEM images were recorded with a Carl Zeiss – Merlin, field emission scanning electron microscope, equipped with a Gemini column and integrated high efficiency In-lens and SE2 detectors, for high spatial/depth-of-field resolution secondary electrons (SE) imaging of surface structure and topography. The microscope was used in high vacuum and high-resolution acquisition mode and the images were acquired at an accelerating voltage of 5 kV and a few seconds frame-integration time, in order to minimize charging effects and sample damages. The hydrogels were cut, frozen and lyophilized prior to be imaged. The pore size was determined by taking 50 random pores followed by statistical analysis using ImageJ software (NIH, United States).

Stability test . The analysis was carried out keeping the hydrogels either in PBS or DMEM at 37 °C, and at determined time points (up to 7 days) the weight was measured. The stability of the hydrogels was then measured as residual weight percentage:

$$Rw\% = \frac{w - w_0}{w_0} 100\%$$

where w_0 is the starting weight of the hydrogel at t = 0, and w is the weight at each time point. The measure was repeated three times and the data are reported as the average of the three measures.

Swelling Behaviour . The swelling property of the hydrogels was determined by using a conventional gravimetric method (N. Gallo et al., 2020). Briefly, the dry weight of hydrogels was recorded prior to immerse them in PBS at 37 °C. Then, the swelled weight of hydrogels was taken at various time points up to 48 h. The swelling behaviour was estimated as the swelling ratio percentage using the following equation:

$$Sr\% = \frac{w_s - w_d}{w_d} 100\%$$

where w_d is the dry weight of the hydrogel and w_s is the wet weight after hydration in PBS.

Collagen Release via BCA assay . The A-C hydrogels were kept in PBS at 37 °C and at determined time intervals the volume of buffer (equal to 1 mL) was collected to estimate the protein content via BCA assay (Terzi et al., 2018). A calibration curve was set using collagen solutions at known concentrations. For each time interval, a blank sample (i.e. the PBS collected from agarose hydrogels prepared without collagen) was measured too.

Fourier-transformed infrared (FTIR) spectroscopy . The measurements were performed on the A-C hydrogels at the different collagen ratios (0.125%, 0.25%, and 0.50%) directly deposited on the ATR crystal. FT-IR

spectra were recorded in transmittance mode on a Jasco 6300 spectrometer (Jasco Corp., Tokyo, Japan) between 4000 and 500 cm^{-1} with 40 scans and a resolution of 4 cm^{-1} and analyzed with the Spectra Manager software (Jasco). The spectrum of each sample was acquired against a background obtained with the crystal without any sample. All analyses were carried out at room temperature.

2.3 Mechanical properties

The effect of the agarose concentration on the Young's modulus of the agarose-collagen hydrogels was evaluated by uniaxial compression test. The correlation with time and temperature was also investigated. Briefly, the hydrogel samples were incubated in PBS at 37 °C in a humidified atmosphere with 5% CO_2. At fixed time points (0, 1, 4, and 8 days), cylinders of 8 mm were punched out and loaded into the testing chamber. All tests were performed with a universal testing machine ZwickiLine (Zwick Roell, Germany) fitted with 10 N load cell. Loaded samples were hydrated in PBS at 37 °C and subjected to compression with a displacement rate of 0.01 mm/s, until 80% strain (L. C. Gallo et al., 2018; Monaco, Cholas, Salvatore, Madaghiele, & Sannino, 2017). The compressive modulus was calculated by linear fitting between 2 and 10% of strain of the stress-strain curve. The test was performed in triplicate for each sample type and time point.

2.4 Diffusion test

PBS solutions containing either FITC-labelled Hyaluronic acid (10kDa molecular weight) or Transferrin-TRITC (80 kDa molecular weight) at known concentration were prepared and deposited over the A-C hydrogels. The photoluminescence signal of the loaded solutions was recorded over time and the resulting concentration was extrapolated from a calibration curve. The diffusivity of the two molecules within the hydrogels was assessed determining the ratio between the concentration of the fluorescent molecule (either hyaluronic acid or transferrin) at the analyzed time point and that measured in free PBS.

2.5 Cell culture conditions and tumor spheroid preparation

Human tumor cells were purchased from the American Type Culture Collection (ATCC). The human breast cancer cell lines MCF-7, MDA-MB-361, MDA-MB-231 and the human neuroblastoma SH-SY5Y cells were cultured as 2D monolayers in DMEM medium (4500 mg/L glucose) supplemented with 10% FBS, 100 U/mL penicillin and 100 µg/mL streptomycin at 37 °C in an atmosphere of 5% CO_2.

The cells were trypsinized, counted and added to the A-C blend at a density of $2.5x10^4$ cells/mL in complete growth medium. The cell suspension containing agarose and collagen was let to gel into the well plate. Then, 1 mL of DMEM was added over the cell-embedded hydrogels prior to transfer the plate into the incubator. The medium was changed every 4 days.

Morphological analysis of the tumor spheroids.

The progressively developing spheroids were observed at 24 h intervals. The morphological characteristics of spheroids including their diameter and shape were measured by optical analysis using a EVOS XL Cell Imaging System microscope (Thermo Fisher, Waltham, MA USA). The mean diameter of the 3D structures was calculated by using ImageJ Software (1.48v).

For SEM imaging the tumor spheroids embedded within the hydrogels were fixed with glutaraldehyde (2.5%) in cacodylate buffer (0.1 M) at 4 °C O.N. The fixed specimens were washed three times with PBS, and 1% osmium tetroxide in a cacodylate buffer was added for 6 h. Then, the samples were washed three times with PBS, cut and lyophilized. Finally, the as-prepared samples were transferred to the SEM microscope to be imaged. The operating conditions of the microscope were the same as those used for imaging the hydrogels.

2.6 Cellular assays

Live/Dead assay . Viability of spheroids was qualitatively analyzed using a Live/Dead assay kit (Thermo Fisher Scientific, Inc.). The activity of intracellular esterase induces non-fluorescent, cell-permeant calcein acetoxymethyl to become fluorescent, giving the viable spheroids a green fluorescence. Ethidium homodimer enters and binds to nucleic acids only into damaged cell producing a red fluorescence thus indicating dead

cells. The assay was performed at three time points to monitor the viability of the spheroids during their growth. In detail, the medium was removed from the plates containing the spheroids-embedded hydrogels. The samples were washed twice with PBS. Then, a phosphate buffer solution containing calcein and ethidium homodimer at the concentration suggested by the supplier company was added to the plate that was kept in incubation at 37 °C for 1 h. Finally, the solution was replaced with fresh PBS prior to image the samples under a Fluorescence Microscope (EVOS FLoid Cell Imaging Station, ThermoFisher, Waltham, MA USA).

Mitochondria toxicity assay. MitoTracker Red from Life Technologies was dissolved in PBS and added to the hydrogel containing the spheroids at the 5^{th} day of growth (working concentration: 250 nM). The samples were kept in incubation for 1 h at 37 degC and then imaged under a Fluorescence Microscope (EVOS FLoid Cell Imaging Station, ThermoFisher, Waltham, MA USA).

Cisplatin treatment. MCF-7 spheroids were grown in 0.25%-0.02% and 0.125%-0.02% A-C hydrogels up to 12 days. Then, a DMSO solution of cisplatin was added to the spheroids-embedded hydrogels to reach a final concentration equal to 100 μM. After 24 h incubation the medium was removed and the hydrogels were carefully rinsed with fresh medium prior to perform the Live/Dead assay (Thermofisher), as already reported.

2.7 Immunofluorescence microscopy analysis. After 5 days of growth within the hydrogels, the spheroids were fixed with ice-cold 4% paraphormaldehyde for 30 minutes. Then they were washed twice with PBS and incubated with a mouse anti E cadherin (E-cad; Santa Cruz, sc-8426) antibody overnight (O.N.), according to the manufacturer's protocol (1:1000 dilution in PBS). Subsequently, the samples were incubated with an anti-mouse Alexa Fluor 488 (AF488) conjugated secondary antibody (Cell Signaling). The images of fluorescently labelled proteins were captured using a fluorescence microscope (Leica LMD7000, Mannheim, Germany).

2.8 Enzymatic digestion of agarose for spheroids recovery

0.25%-0.02% and 0.125%-0.02% A-C hydrogels containing MCF-7 spheroids at different days of growth were incubated with 40 U of β-Agarase from Pseudomonas atlantica and left under incubation O.N. at 37 °C. Then, the supernatant was collected and observed under an optical microscope to visualize the presence of floating spheroids. Soonafter, the spheroids were fixed with 4% paraformaldehyde and stained with DAPI. The labelled structures were imaged under a Fluorescence Microscope (EVOS FLoid Cell Imaging Station, ThermoFisher, Waltham, MA USA).

2.9 Statistical analysis

All data represent the average value of at least three independent experiments, unless otherwise specified. Normally distributed data was compared with a two-tailed Student's t-test.

3. Results

3.1 Agarose-collagen hydrogel: preparation and characterization

Three agarose-collagen (A-C) weight ratios were used for preparation of the hydrogels used in this paper, i.e. 0.5%-0.02%, 0.25%-0.02%, and 0.125%-0.02%, respectively. The collagen amount (equal to 0.2 mg/mL) was kept constant in all the hydrogel formulations. This concentration, close to that used in other studies in which blended hydrogels were prepared, is sufficient to provide the anchoring sites to the embedded cells. On the other hand, the amount of agarose was varied from 0.5 to 0.125% to evaluate the impact on the biophysical properties of the hydrogel and consequently their effect on the cellular spheroids development. To prepare the hydrogels and, at the same time, to prevent the denaturation of collagen and the cell damage and death, the agarose solution was first heated until boiling (100 °C) to dissolve the polysaccharide, and then cooled down until it reached 45 °C. At this point, since gelation of pure agarose occurs at around 36 °C, it was rapidly mixed with collagen and the cell suspension. The preparation sketch is reported in Figure 1S.

The physical properties of the A-C hydrogels were characterized. The study of the hydrogels surface structure and topology through SEM techniques shows that decreasing the agarose percentage, the porosity of the hydrogels increases and the whole structure appears less compact (Figure 1). In 0.125%-0.02% A-C hydrogels, indeed, the higher percentage of water makes the dry structure very brittle displaying pores that are quite uniform and interconnected with a mean size of 71 ± 14 μm (Figure 1e and f). Although the measure of the pore sizes of a dry structure cannot be considered realistic, it provides an estimation of the 3D organization of the hydrogels. In 0.25%-0.02% and 0.5%-0.02% A-C hydrogels, the number of pores is smaller, while the average pore size appears to be slightly larger (81 ± 21 and 87 ± 25 μm, respectively, Figure 1a-d). The higher turgidity and compactness of the hydrogels with higher percentage of agarose is also evident at a macroscopic level, as shown in the bottom panel of Figure 1S. Indeed, while 0.25%-0.02% and 0.5%-0.02% A-C hydrogels appear self-standing, that with 0.125%-0.02% weight ratio looks softer and less compact.

FTIR spectroscopy was performed on the hydrogels to investigate whether collagen, though the low percentage amounts used, was detectable on the outer surface of the hydrogels, thus confirming its distribution within the hydrogel texture. To this aim, the analysis was performed directly on the synthetized hydrogels deposited on the ATR crystal, without any further manipulation. Pure agarose hydrogel (0.25%) was recorded as reference (light green line in Figure 2a), showing the typical signals at 988 and 1076 cm^{-1}, relative to the C-H bending and to the C-O stretching of the glycosidic bonds, and two broad peaks at 1656 and 3421 cm^{-1}, characteristic of the stretching of the H-O-H bound water and of the O-H hydrogen bonded carbohydrate hydroxylic groups, respectively (Oza, Prasad, & Siddhanta, 2012). Two broad peaks were also observed in the pure collagen hydrogel at about 3328 and 1645 cm^{-1} for the amide C=O and N-H stretching, respectively (pink line in Figure 2a). Additional smaller signals were detected at 1051 $cm^{-1}$for the C-OH stretching vibrations of carbohydrate moieties attached to the protein (Petibois, Gouspillou, Wehbe, Delage, & Déléris, 2006). The resulting FTIR spectrum of the blend 0.25%-0.02% A-C hydrogel (red curve of Figure 2a) showed all the peaks characteristic of the pure compounds, i.e. smaller signals at 989 and 1079 cm^{-1}, with a small side-bump at 1045 cm^{-1}, and much broader peaks at 1649 and 3464 cm^{-1}. Interestingly, while the last two peaks had similar intensity in pure collagen, a much higher intensity of the signal at lower frequencies was observed in pure agarose as well as in the blend hydrogel. As expected, no significant differences were observed in the spectra of the other two blend hydrogels (data not shown).

Another critical feature of a hydrogel is the capability to absorb and retain water. Figure 2b) shows the swelling behavior of the three types of hydrogels. The hydrogels containing 0.5% and 0.25% agarose show a similar trend with a swelling ratio respectively of 20 and 25 times at t_0 and a maximum swelling of 27 and 30 times after 24 h in PBS. These data are in accordance with those reported in the literature. On the other hand, the ability to absorb water of the hydrogel with 0.125% agarose is considerably lower, with a swelling ratio of 5.2 times at t_0 and 7.1 at t_{24}, respectively. Thus, there appears to be a critical threshold of agarose percentage below which the physical properties of the hydrogel are dramatically altered.

A degradation test was carried out to investigate the stability of the three formulations over time. Panels c) and d) of Figure 2 show the percentage residual weight of the hydrogels kept at 37 °C in PBS and DMEM up to two weeks. 0.5%-0.02% and 0.25%-0.02% A-C hydrogels were shown to be quite stable to degradation and lost around 10 and 15% of their weight after 14 days of incubation in PBS and DMEM with 10% FBS, respectively. On the other hand, 0.125%-0.02% A-C hydrogels showed a maximum of degradation close to 40% after 2 weeks in both incubation media.

In parallel, the amount of collagen potentially released was estimated via a protein quantification assay. To this aim, the A-C hydrogels were kept in PBS at 37 °C and the volume of PBS was collected and renewed every 24 h up to 14 days. Figure 2S shows the results of the BCA assay carried out with the three types of hydrogel. Collagen release was detected in all hydrogels but to a higher extent and with a quicker trend in that with a lower agarose content. The overall percentage amount of collagen release after 2 weeks is equal to 50%, 27%, and 8% of the whole collagen present in the hydrogel containing 0.125%, 0.25%, and 0.5% agarose, respectively. This loss, together with the less compact texture of the 0.125%-0.02% A-C hydrogel, would explain the higher degradation of this matrix.

A further parameter that deserves investigation is the capability of a hydrogel to allow the diffusion throughout the matrix of biomolecules and nutrients, such as growth factors and serum proteins having molecular weight of several tens of kDa. To this aim, a diffusion test was performed by using two fluorescent probes, FITC-conjugated hyaluronic acid and Transferrin-TRITC, with a MW of around 10 and 80 kDa, respectively. Once loaded onto the three hydrogel formulations, the variation of concentration of the feeding solution was monitored over time and reported versus the diffusion in pure PBS. The results show that hyaluronic acid (Figure 2e) diffuses rapidly into the softest hydrogel reaching 100% diffusion after 72 h, while the other two hydrogels show a similar trend although with a more gradual diffusion that decreases by increasing the percentage of agarose, reaching a maximum of 82% and 75% after one week, respectively. On the other hand, in the case of transferrin-TRITC the diffusion is much slower: in the 0.125%-0.02% A-C hydrogel the diffusion reaches almost 48% after 24 h, while at the same time point it is closed to 10% in the case of the other two blends. (Figure 2f) Noteworthy, after one week the diffusivity does not exceed 50% even in the softest matrix.

The structural properties of the A-C samples were also evaluated by mean of compression test under physiological-like conditions (PBS, 37 °C). Figure 3a) shows how the agarose concentration deeply affects the hydrogels' mechanical properties. In fact, the increase in agarose concentration corresponds to an increase in the compressibility modulus. As expected, the 0.5%-0.02% ratio shows the highest E modulus (5.7 ± 0.5 kPa), followed by 0.25%-0.02% (1.6 ± 0.4 kPa) ($p = 0.0004$) and 0.125%-0.02% (0.7 ± 0.2 kPa) ($p = 0.0001$). A minor but significant difference was found between 0.25%-0.02% and 0.125%-0.02% ($p = 0.03$). In order to correlate degradation resistance to structural stability over time, the A-C samples' mechanical performances were evaluated after 0, 1, 4, and 8 days of incubation in physiological-like conditions (PBS, 37 °C, in humified atmosphere with 5% CO_2). While 0.125%-0.02% hydrogels could not be tested over time due to their low consistence, the 0.5%-0.02% and 0.25%-0.02% blends retained their structural integrity until the 8^{th} day of measure. As shown in Figure 3b, no significant changes in the E modulus were registered in the case of 0.5%-0.02% and 0.25%-0.02% hydrogels. These data are in accordance with the degradation tests in which a minimum weight loss was recorded.

3.2 Growth of mammary spheroids in A-C hydrogels

We generated mammary spheroids from three different breast cancer cell lines. We focused on luminal estrogen receptor positive cells, MCF-7 and MDA-MB-361, and a triple negative model (MDA-MB-231) for comparative analysis. To start, cells were seeded at the density of 2.5 x 10^4 per mL inside the three types of hydrogels and time course studies (up to 14 days) were performed to monitor the process of multicellular spheroid formation. MCF-7 and MDA-MB-361 formed spheroids successfully in all the three types of hydrogels. On the other hand, MDA-MB-231 did not form spheroids in any of the hydrogel conditions. As shown in Figure 3S, MDA-MB-231 cells start to replicate during the first days without reaching a defined 3D organization.

As reported, MCF-7 and MDA-MB-361 cells formed spheroids, but the size and the morphology of the 3D structures was not the same in all the conditions tested. Figure 4 and 4S show the spheroids at different days of growth in the three types of hydrogels. In the stiffer ones the spheroids were spherical but smaller (Figure 4S) than those grown in the other two conditions (Figure 4), especially in the case of MDA-MB-361 cells. This effect is more evident as the 3D structure progressively grows over time: the average size of MDA-MB-361 derived spheroids after 12 days growth in hydrogels with 0.5% agarose was around 63.1 ± 7.8 μm, while it reached 81.3 ± 6.3 μm and 94.7 ± 9.5 μm in 0.25%-0.02% and 0.125%-0.02% A-C hydrogels, respectively (Table 1S). In the case of MCF-7 cells, the size gap was of about 7 and 27 μm respectively, being the spheroids at 12 days about 64 μm large in the hydrogels with 0.5% agarose, while they reached a diameter of about 70 μm in the 0.25%-0.02% hydrogel and 91 μm in the softer ones (Table 1S). The images of Figure 4 clearly evidence how the 3D structures evolve from a single cell over time, and the growth curves reported in the lower panels of the Figure show that while in the hydrogel with 0.25% agarose the spheroids look to reach the growth stabilization at 14 days, in the softest environment they still display a positive growth trend. Thus, though this study is focused to the analysis of the spheroids growth within two weeks,

that is a time range sufficient for drug testing, we prolonged the observation time up to 28 days to point out the growth curve of the 3D cell structures in the 0.125%-0.02% A-C hydrogels. As shown in lower panels of Figure 5S, in the softest matrix the spheroids continued to grow exceeding the 100 μm diameter in both cell lines at 28 days. On the other hand, in the 0.25%-0.02% A-C hydrogels the spheroids stop their growth and after 4 weeks they started to shrink and appear senescent with dark cellular stuff. In this sense, it looks that the softest hydrogel is capable of sustaining the spheroids growth for longer time, and, especially in the case of MCF-7, the spheroids display irregular contours and looser structure. As a general consideration, we observed that MCF-7 tolerate stiffer environments as compared to MDA-MB-361. Indeed MCF-7 generated small spheroids in hydrogels with 1% agarose too (Figure 6S), while MDA-MB-361 did not.

Therefore, the hydrogel stiffness and the matrix composition regulate the spheroids growth and morphology and, more interestingly, affect the local migration of the outer cells. Indeed, as shown in Figure 5, only the softest matrix is able to induce protrusion of cells from the outer layer and their local dissemination. As already reported, the motility of these cells depends on the interaction with the microenvironment, mainly with collagen (Nguyen-Ngoc et al., 2012). It is likely that the hydrogels with 0.125% agarose promote the protrusive behavior while collagen provides the anchoring point for the spatial dissemination of the cells. The reduced migration of the outer cells in the hydrogels with 0.25% agarose should be related to the tighter pressure that the matrix exerts on the cells, leading, as already described, to more compact spheroids.

Based on these observations and with the aim to study the effects of the mechanical features of the environment on the tumoroids features, the following analyses were carried out comparing the two conditions (0.25% and 0.125% agarose-based hydrogels) in which both cell lines were able to form healthy and stable spheroids up to two weeks.

3.3 Mammary spheroids viability and epithelial markers expression

The viability of the spheroids obtained from the MCF-7 and MDA-MB-361 cell lines in both type of hydrogels was qualitatively analyzed through a Live/Dead fluorescence assay that evidence the cell viability even after 14 days of growth (Figure 7S). Indeed, at 8 days the homogeneous green fluorescence evidenced that all the cells of the spheroids were viable; after 14 days few red spots were visible in the 3D structure grown in the matrix with 0.25% agarose, showing their initial aging, while the spheroids embedded in the softer hydrogel resulted absolutely viable. These data are in accordance with the previous analysis of the growth curves of the 3D structures in the two systems. To further confirm this trend, the assay was also performed after 28 days. Notably, while the spheroids grown in the 0.125% agarose-based hydrogels were still viable, those prepared in the stiffer matrix were dead. Furthermore, Mitotracker red, an indicator of mitochondrial membrane potential able to selectively stain live mitochondria, was used to gain deeper insights into the status of cells and the porosity of the hydrogels (Figure 6). Mitotracker staining showed the presence of live mitochondria in the periphery as well as in the center of the spheroids, thus proving the permeability to oxygen of the A-C hydrogels, since mitochondrial function critically depends on its availability.

We then determined by immunofluorescence the expression of E cadherin, a typical epithelial marker in 3D spheroids. Fig 7 clearly shows that mammary spheroids maintain the expression of the transmembrane glycoprotein E-cadherin and clearly demonstrate the presence of tight cell-cell interactions, both typical features of an epithelial phenotype (Figure 7). Overall, these data suggest that our hydrogel is a suitable method for the generation of mammary spheroids.

To further elucidate the morphology of the spheroids and their arrangement into the hydrogel, ultrastructural analysis of MCF-7 spheroids was performed showing their 3D structure that looks enveloped into the hydrogel matrix: the protrusion of the spheroids from the hydrogel can be clearly appreciated and they can be compared to cocoons anchored to a branch (Figure 8S).

3.4 Cisplatin delivery to the embedded spheroids

To evaluate the exploitation of these 3D systems as a drug-screening platform, the MCF-7 spheroids embedded either in the 0.25%-0.02% or 0.125%-0.02% A-C hydrogels were treated with 100 μM cisplatin. After

24 h incubation, the Live/Dead assay was performed and the samples were analysed under the fluorescence microscope. The images of Figure 8 show that the dead cells were detected in the hydrogels administered with cisplatin, while control samples were brightly green fluorescent. The analysis of the distribution of the fluorescent pixels performed on 25 spheroids for each type of sample evidenced that the difference between the number of dead cells of the control and those of the drug-treated samples is statistically significant ($p < 0.01$) (Figure 8, lower panel). Furthermore, it looked that the penetration of the drug depended on the agarose percentage amount, as indeed, the number of dead cells was higher in the hydrogels containing 0.125% agarose. Interestingly, when the samples, after 24 h incubation with the drug, were kept in fresh medium for additional 5 days and then observed under the microscope, the structure of the spheroids was dramatically altered. A huge number of dead cells peeled off from the spheroids and many cellular debris were spread into the matrix while small residues of the 3D structures were still visible (Figure 9S). This effect was observed in both types of matrices at 5 days post drug treatment.

3.5 Enzymatic digestion of agarose for spheroids recovery

We intended to evaluate the possibility to recover the spheroids from the hydrogel matrix. for further processing and/or other biological studies To assess the degradability of the A-C hydrogels, the blends with 0.25% and 0.125% agarose containing MCF-7 spheroids at different days of growth were incubated with β-Agarase from Pseudomonas atlantica (Malmqvist, 1978)(Fu & Kim, 2010). After O.N. incubation at 37 °C with 40 U Agarase, in the case of 0.25% blended hydrogels only the spheroids located in the outer layer of the hydrogel were recovered (upper panels of Figure 10S). Most of the hydrogel remained intact and the spheroids continued to growth within as in control hydrogels not treated with Agarase. On the other hand, in the case of the softest matrices, containing 0.125% agarose, all the tumoroids were recovered after Agarase treatment (lower panels of Figure 10S). Indeed, after O.N. treatment, the hydrogel was completely dissolved. Noteworthy, as shown in the stability test (Figure 2), the hydrogels with 0.125% agarose showed a spontaneous higher degradation than those with 0.25%. Thus, the addition of agarose boosted the degradation process leading to the complete dissolution of the softer matrix. The images of Figure 10S show the morphology of the spheroids collected after Agarase treatment in both types of hydrogels at different times of growth. Furthermore, the recovered tumoroids were fixed and their nuclei stained with DAPI to show their suitability for further processing and studies. As reported in Figure 9, some free individual cells, detached from the surface of the spheroids, can be observed, likely due to the centrifugation steps performed for the staining protocol. Nevertheless, the spheroids preserve their shape and their morphology.

4. Discussion

In this work blended hydrogels composed of agarose (variable weight amount from 0.125 to 0.5%) and collagen (fixed weight amount equal to 0.02%) were prepared as enabling matrices for the growth of 3D cellular structures. They combine the biomechanical properties of agarose and the bioadhesivity of collagen. The amount of collagen is 6.25-, 12.5- and 25- times lower than that of agarose, and the formation of the hydrogel is ascribed only to agarose and not to collagen. Indeed, although the self-assembling capability of collagen molecules *in vitro* under physiological conditions is well known, reconstituted collagen fibrils, that are held together by non-covalent interactions (hydrogen bonding, hydrophobic and electrostatic interactions), are free to slide and do not form a stable 3D network (Tian, Liu, & Li, 2016).

The characterization of the hydrogels evidenced that the agarose percentage governs the morphological, structural and mechanical features of the matrix. Reasonably, higher the agarose amount, stiffer the hydrogel results. On the other hand, the lowest agarose amount corresponds to the fastest degradation and diffusion of molecules through the matrix. The higher degree of degradation of the softest hydrogel is also associated to a higher release of collagen. Noteworthy, the collagen is simply entrapped within the hydrogel mesh and not chemically linked to the agarose backbone. Thus, it can be expected that a less compact hydrogel facilitate the release of collagen, as determined by the protein quantification assay. These findings are in accordance with the compression tests that evidenced a significant reduction of the E modulus as the agarose amount shifted from 0.5 (5.7 ± 0.5 kPa) to 0.25 (1.6 ± 0.4 kPa) up to 0.125 (0.7 ± 0.2 kPa). Presumably, a higher amount of agarose allows, during the cooling down phase after synthesis of the hydrogels, the formation of

more and tighter hydrogen bonds that reflect the higher structural stability observed visually because of the increase in the compression modulus.

Similarly, the entry and movement of biomolecules through the blended hydrogel looks to be associated to the agarose percentage. The bigger the biomolecule and the stronger the type of non-covalent interactions it can establish with the matrix the slower they are, and that the total amount that may reach the cells embedded into the matrix is only a fraction of the feeding solution. In this sense, the hydrogel may act as a physical barrier to the diffusive transport of specific nutrients and drugs to the tumoroid, similarly to what occurs *in vivo*(Monteiro, Gaspar, Ferreira, & F., 2020).

The formation and the growth of tumoroids from three breast cancer cell lines, namely MCF-7, MDA-MB-361 and MDA-MB-231 cells, were investigated upon variation of the agarose concentration of the matrix. While MCF-7 and MDA-MB-361 formed 3D structures, whose size and compactness is strictly related to the stiffness and thus to the percentage of agarose of the surrounding matrix, MDA-MB-231 cells, a triple negative breast cell line, did not, in accordance with previous findings (Iglesias et al., 2013; Tasdemir, Bossart, Li, & Zhu, 2018).

The inability of this cell line to form spontaneously tumor spheroids is probably consistent with their lack of adherens junctions.

In detail, we observed that after lading individual cells into each of the three blended hydrogels, both cell lines formed spheroids. By analysing the size and morphology of the structures, we realized that breast cancer cells prefer hydrogels with a stiffness from 1.5 to 0.7 kPa, while stiffer matrices, as those with 0.5% agarose,did not result suitable to support the growth of the spheroids. We reasoned that a different tissue-specific tropism of the cellular models probably contribute to this result. In this case, MCF-7 cells have a low metastatic potential, and are not tissue-specific, while MDA-MB-361 cells were derived from a brain metastasis. The growth of MDA-MB-361 cells on a softer hydrogel matches more closely their *in vivo*metastatic microenvironment. This was in part confirmed when we examined the growth of a neural cell model. In A-C 0.125%-0.02% hydrogel, the neuroblastoma SH-SY5Y cells generated spheroids in a time-dependent manner and their size was bigger than when grown in the stiffer 0.25%-0.02% hydrogels (Figure 11S). As a general remark, SH-SY5Y spheroids reached larger diameters (121.7 ± 14.2 μm) than those obtained with MCF-7 and MDA-MB-361 grown in the same matrix, and this evidence could be related to the different origin of the cell line.

The Live/Dead assay and the mitochondrial staining showed that the spheroids are viable up to 14 days in both types of hydrogels. Notably, we monitored the 3D cultures up to one-month: the spheroids continued to grow in the softer hydrogel, reaching an average size of around 100 μm. On the other hand, in the 0.25%-0.02% hydrogels the spheroids stopped their growth after 2 weeks and started to senesce resulting definitely dead after 4 weeks. This different behavior might be related to the interactions between the cells and the surrounding environment as the 3D structure grows over time: the limited degradation and capability of the stiffer hydrogels to accommodate the spheroids induce their slow aging and death.

These results confirm that soft agarose-collagen hydrogels allow 3D long-term cell growth although cells derived from different tissues sense the change in stiffness of the substrate and significantly modify their behaviour. It has been shown, in this respect, that cells respond to ECM environment by regulating a plethora of transcription factors and other signals that affect cytoskeleton, cellular uptake, cell cycle that in turn determine their morphology, proliferation, differentiation, tumor invasion and metastasis (Kruger et al., 2019; Ranamukhaarachchi et al., 2019; Trappmann et al., 2012; Wang, Gong, Zhang, & Fu, 2017). Among them, it is worth mentioning the transmembrane glycoprotein E-cadherin that is expressed in epithelial cells and connect them through lateral adherent junctions. It has been demonstrated that the level of expression of cadherin represents a crucial feature in cancer progression as it is involved in the epithelial-mesenchymal transition (Wong, Fang, Chuah, Leong, & Ngai, 2018). Loss of E-cadherin expression is generally associated to the lack of intercellular contacts and to increased tumor cell invasiveness via activation of the signalling pathways that regulate metastatic progression (Vergara et al., 2016). E-cadherin expression is also associated

to the formation of multicellular tumor spheroids, as already demonstrated (Cui et al., 2017). Indeed, the spheroids derived from MCF-7 and MDA-MB-361 displayed the expression of E-cadherin, as shown in Figure 7.

As a general consideration, softer hydrogels allow for the establishment of long-term culture of large and irregular breast tumor spheroids, while stiffer environment condition the growth of small and compact 3D cell strictures for shorter periods (Figure 12S).

Finally, we showed the possibility to recover the tumoroids from the hydrogel after treatment with Agarase enzyme. The yield of the recovery process is quantitative and highly reproducible in the softest gel that undergoes spontaneously to degradation, while in the matrix with 0.25% agarose only a small percentage of 3D structures can be successfully recovered for further biological and biomolecular studies.

5. Conclusion

A simple and cost-effective method for the generation of tumor spheroids has been reported. It consists of enveloping individual tumor cells in agarose hydrogels (with 0.25 or 0.125% weight percentage) blended with 0.02% collagen, where agarose reproduces the biomechanical features of the ECM, while collagen provides the anchoring sites for the membrane proteins. The growth of tumoroids deriving from three breast cancer cells lines was analyzed and compared. Interestingly, one cell line, MDA-MB-231 did not form spheroids in any of the conditions employed, while the other two lines, MCF-7 and MDA-MD-361displayed a quite similar behavior.

The variation of the agarose amount affected the physical and mechanical features of the resulting hydrogel and the growth of spheroids. Indeed the stiffer the hydrogel, more compact and slightly smaller the tumoroids resulted. Therefore, depending on the type of tumoroids to be prepared and studied, the hydrogel composition can be easily tuned. The growth of the spheroids was monitored up to 2 weeks, and the qualitative analysis of their viability evidenced few dead cells only after 14 days.

Preliminary drug testing studies with cisplatin show that the blended hydrogels allow following the response of the spheroids to the drug administration. This aspect makes the system potentially useful for routine drug screening**.**

Finally, the degradability of the hydrogels upon enzymatic treatment was demonstrated, leading to complete recovery of tumoroids in the case of the softest hydrogels, while to a partial recovery in the hydrogel with 0.25% agarose. The possibility to recover the spheroids is of a paramount importance as it enables further biomolecular studies with the collected samples.

Conflicts of interest

The authors declare that there are no conflicts of interest.

Acknowledgements

The authors would like to acknowledge the support of the following Italian projects: Progetto Regionale “Lab on a Swab (cod. OTHZY54)”, ”Tecnopolo per la medicina di precisione” (TecnoMed Puglia) - Regione Puglia: DGR n.2117 del 21/11/2018 (CUP: B84I18000540002), and ”Tecnopolo di Nanotecnologia e Fotonica per la medicina di precisione” (TECNOMED) - FISR/MIUR-CNR: delibera CIPE n.3449 del 7-08-2017 (CUP: B83B17000010001).

Figure 1

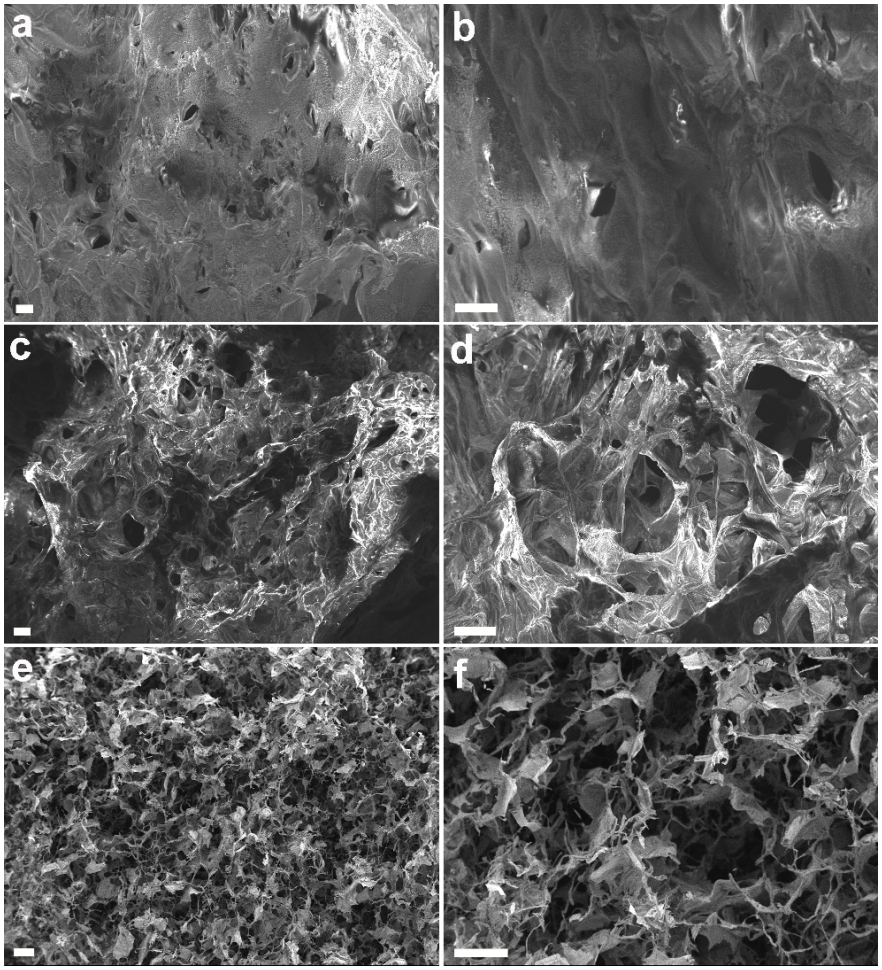

Figure 2

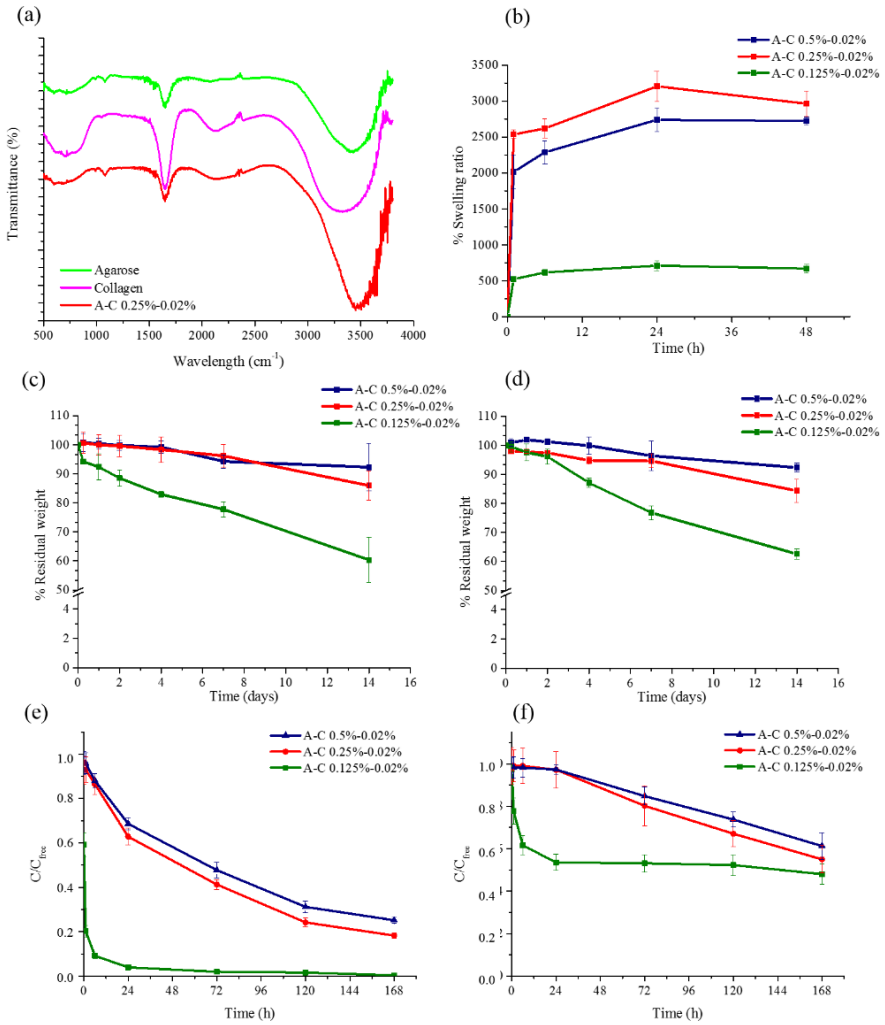

Figure 3

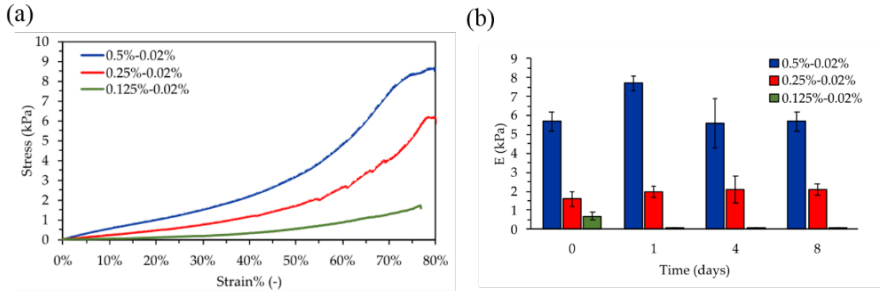

Figure 4

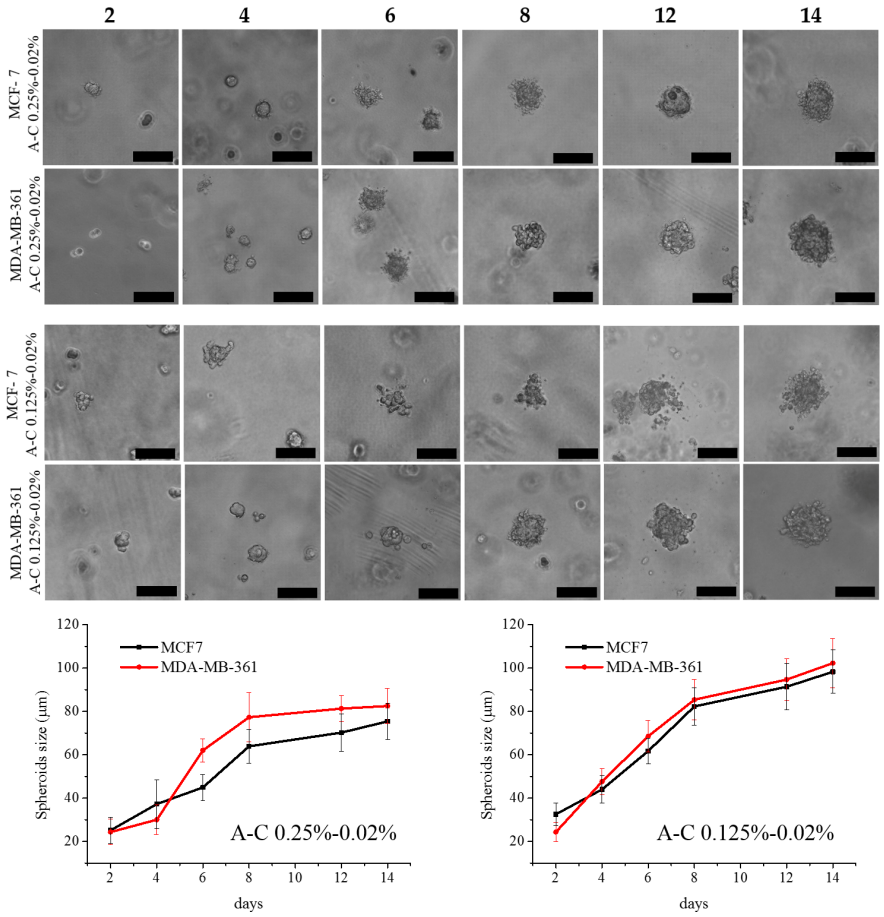

Figure 5

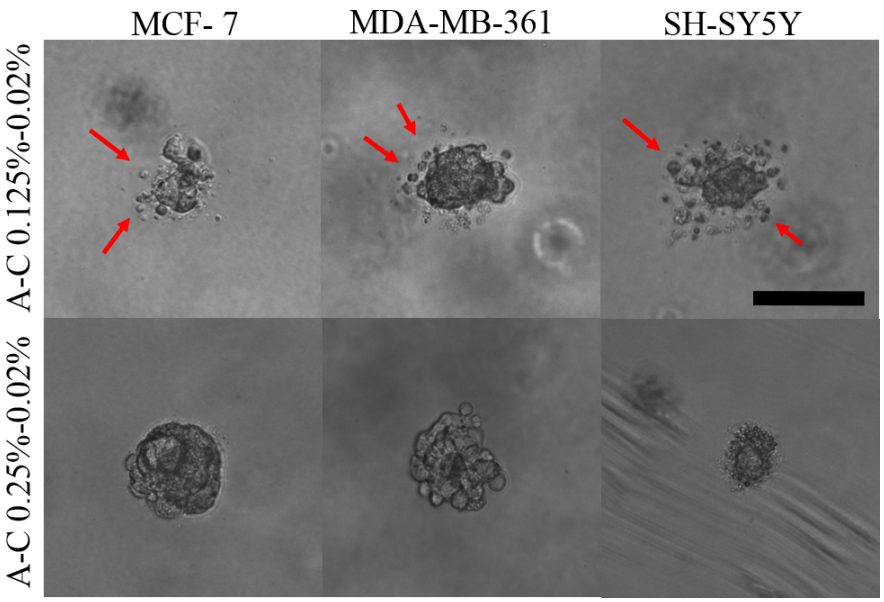

Figure 6

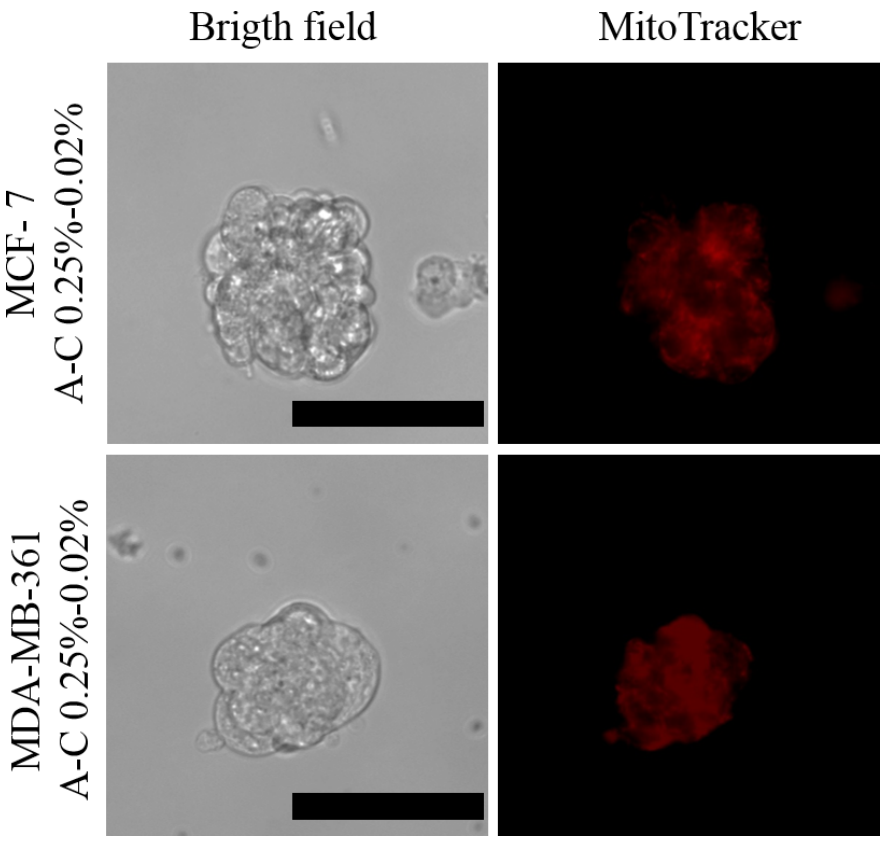

Figure 7

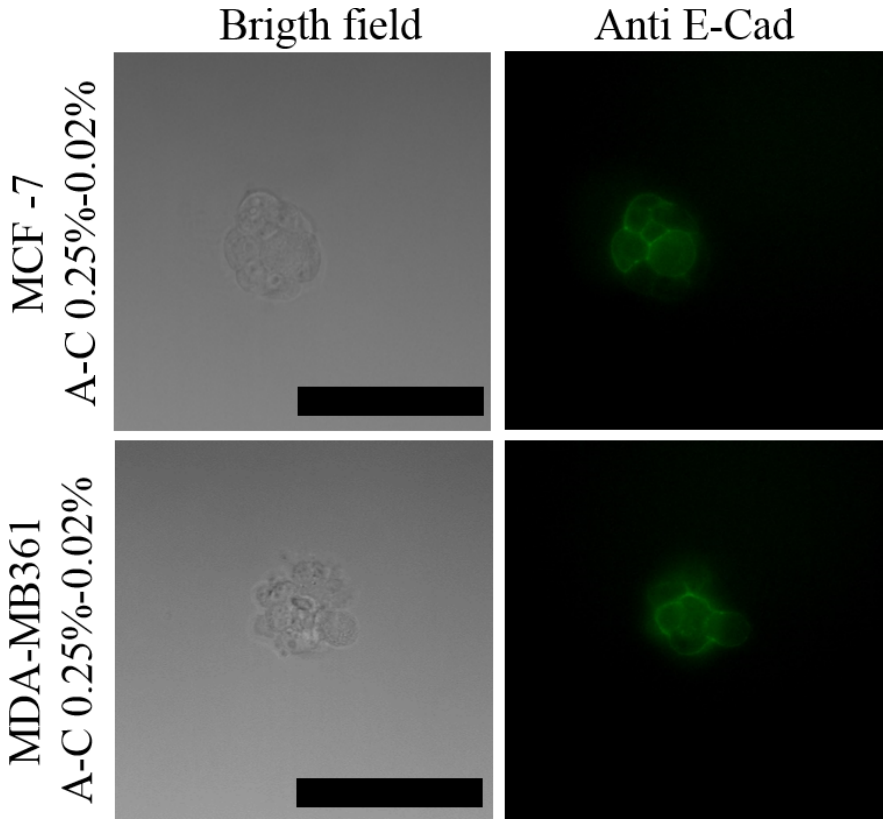

Figure 8

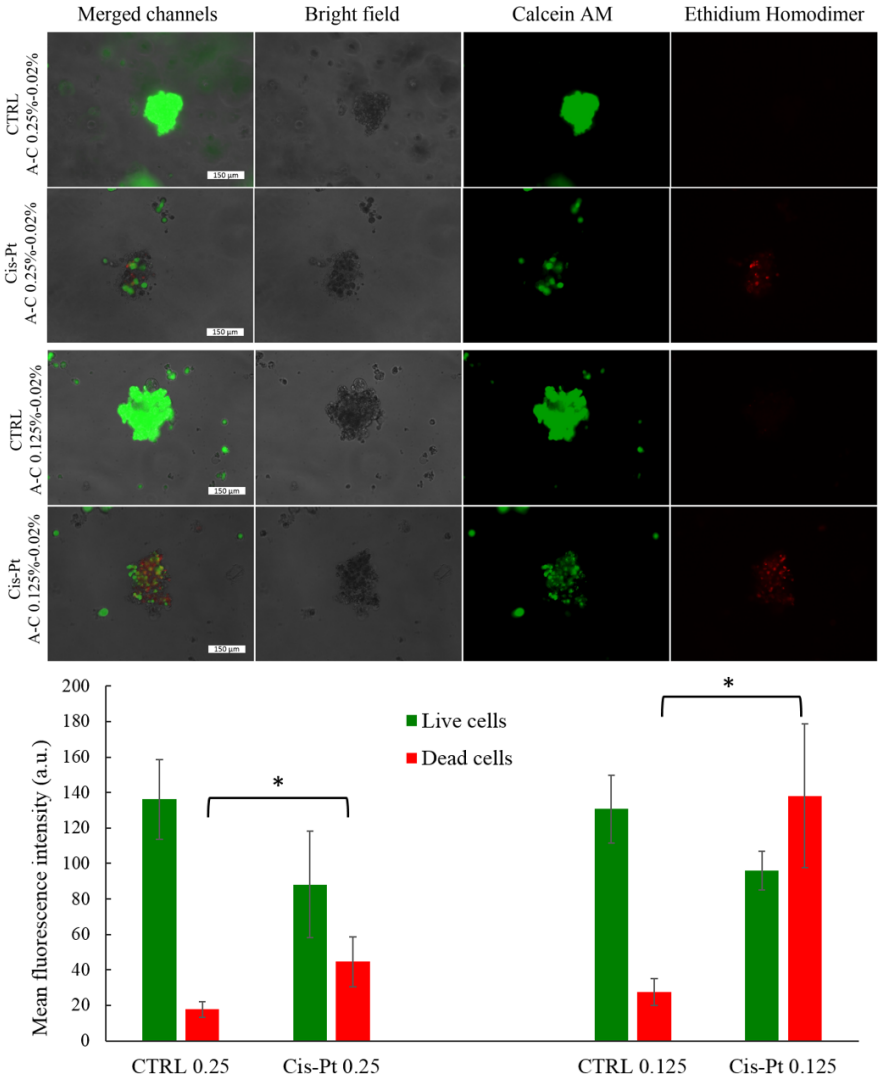

Figure 9

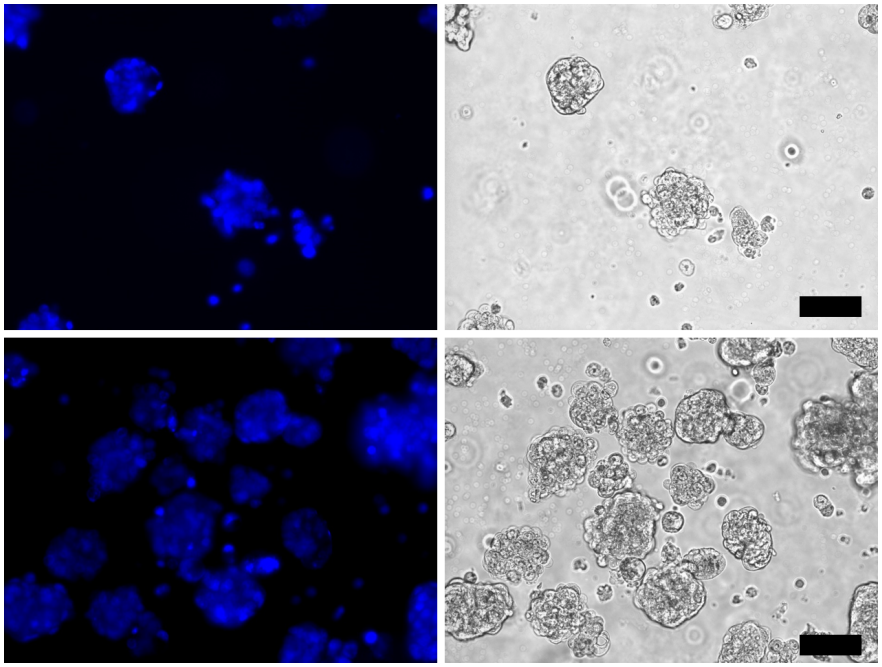

Legends to figures

Figure 1. SEM images at lower (a, c, e) and higher (b, d, f) magnification of the A-C hydrogels at different weight ratios: a-b) 0.5%-0.02%; c-d) 0.25%-0.02%; e-f) 0.125%-0.025%. Scale bar is 100 μm.

Figure 2. a) FTIR spectra of a hydrogel of only agarose (green curve), collagen (pink curve) and a 0.25%-0.02% A-C hydrogel (red curve). b) Swelling behaviour of the A-C hydrogels kept in PBS at 37 °C. c-d) Degradation curves of the A-C hydrogels in PBS and in DMEM medium with 10% FBS, respectively, up to 2 weeks. e-f) Diffusion tests performed with Hyaluronic acid-FITC and Transferrin-TRITC, respectively, up to one week.

Figure 3. Representative stress-strain curves of A-C hydrogels subjected to unconfined compression with a displacement rate of 0.01 mm/s, until 80 % strain (A); Compressive moduli of A-C hydrogels at 0, 1, 4, 8 days of incubation in PBS at 37 °C, in humified atmosphere with 5% CO2 (B). Values represent mean ± SD, where n = 3.

Figure 4. The upper panels show the morphology and the size of the spheroids obtained with MCF-7 and MDA-MB-361 cells grown in 0.25%-0.02% and 0.125%-0.02% A-C% hydrogels, respectively, from 2 to 14 days. The graphs report the growth trend of both cell lines.

Figure 5. Images of the tumor spheroids obtained with MCF-7, MDA-MB-361 and SH-SY5 after 8 days growth in 0.125%-0.02% A-C% (upper panels) and 0.25%-0.02% hydrogels (lower panels). The arrows point to the disseminating cells of the spheroids grown in the soft matrix. Scale bar is 100 μm.

Figure 6. Mitochondrial labelling of living spheroids after 5 days growth with Mitotracker red. Spheroids of MCF-7 and MBA-MB-361 were stained and compared. Scale bar is 50 μm.

Figure 7. Staining of E-cadherin in cellular spheroids of MCF-7 and MBA-MB-361 after 5 days growth in A-C hydrogels. Scale bars correspond to 57.6 μm.

Figure 8. Live dead assay performed with the MCF-7 spheroids embedded into the A-C hydrogels after 24 h incubation with cisplatin. The upper panels refer to the 0.25%-0.02% A-C hydrogels, while the lower panels to those with 0.125%-0.02% A-C ratio. The graph reports the number of live and dead cells in each sample

estimated through the distribution of the fluorescence signals of Calcein AM and Ethidium Homodimer, respectively.

Figure 9. Images of MCF-7 spheroids grown within 0.25-0.02% (upper panels) and 0.125-0.02% (lower panels) A-C matrices, respectively, recovered after Agarase treatment, fixed and stained with DAPI.

References

Anderson, D. E., & Johnstone, B. (2017). Dynamic Mechanical Compression of Chondrocytes for Tissue Engineering: A Critical Review. *Front Bioeng Biotechnol, 5* , 76. doi:10.3389/fbioe.2017.00076

Butcher, D. T., Alliston, T., & Weaver, V. M. (2009). A tense situation: forcing tumour progression. *Nature Reviews Cancer, 9* (2), 108-122. doi:10.1038/nrc2544

Caliari, S. R., & Burdick, J. A. (2016). A practical guide to hydrogels for cell culture. *Nature methods, 13* (5), 405-414. doi:10.1038/nmeth.3839

Cambria, E., Brunner, S., Heusser, S., Fisch, P., Hitzl, W., Ferguson, S. J., & Wuertz-Kozak, K. (2020). Cell-Laden Agarose-Collagen Composite Hydrogels for Mechanotransduction Studies. *Frontiers in Bioengineering and Biotechnology, 8* (346). doi:10.3389/fbioe.2020.00346

Cui, X., Hartanto, Y., & Zhang, H. (2017). Advances in multicellular spheroids formation. *Journal of The Royal Society Interface, 14* (127), 20160877. doi:doi:10.1098/rsif.2016.0877

Davidenko, N., Hamaia, S., Bax, D. V., Malcor, J. D., Schuster, C. F., Gullberg, D., . . . Cameron, R. E. (2018). Selecting the correct cellular model for assessing of the biological response of collagen-based biomaterials. *Acta Biomater, 65* , 88-101. doi:10.1016/j.actbio.2017.10.035

Davidenko, N., Schuster, C. F., Bax, D. V., Farndale, R. W., Hamaia, S., Best, S. M., & Cameron, R. E. (2016). Evaluation of cell binding to collagen and gelatin: a study of the effect of 2D and 3D architecture and surface chemistry. *J Mater Sci Mater Med, 27* (10), 148. doi:10.1007/s10856-016-5763-9

Fu, X. T., & Kim, S. M. (2010). Agarase: review of major sources, categories, purification method, enzyme characteristics and applications. *Marine drugs, 8* (1), 200-218. doi:10.3390/md8010200

Gallo, L. C., Madaghiele, M., Salvatore, L., Barca, A., Scialla, S., Bettini, S., . . . Sannino, A. (2018). Integration of PLGA Microparticles in Collagen-Based Matrices: Tunable Scaffold Properties and Interaction Between Microparticles and Human Epithelial-Like Cells. *International Journal of Polymeric Materials and Polymeric Biomaterials, 69* (3), 137-147. doi:10.1080/00914037.2018.1552857

Gallo, N., Lunetti, P., Bettini, S., Barca, A., Madaghiele, M., Valli, L., . . . Salvatore, L. (2020). Assessment of physico-chemical and biological properties of sericin-collagen substrates for PNS regeneration. *International Journal of Polymeric Materials and Polymeric Biomaterials* , 1-11. doi:10.1080/00914037.2020.1725755

Guimarães, C. F., Gasperini, L., Marques, A. P., & Reis, R. L. (2020). The stiffness of living tissues and its implications for tissue engineering. *Nature Reviews Materials, 5* (5), 351-370. doi:10.1038/s41578-019-0169-1

Hamaia, S., & Farndale, R. W. (2014). Integrin Recognition Motifs in the Human Collagens. In D. Gullberg (Ed.), *I Domain Integrins* (Vol. 819, pp. 127-142).

Iglesias, M. J., Beloqui, I., Garcia-Garcia, F., Leis, O., Vazquez-Martin, A., Eguiara, A., . . . Martin, A. G. (2013). Mammosphere formation in breast carcinoma cell lines depends upon expression of E-cadherin. *PloS one, 8* (10), e77281. doi:10.1371/journal.pone.0077281

Kruger, T. M., Bell, K. J., Lansakara, T. I., Tivanski, A. V., Doorn, J. A., & Stevens, L. L. (2019). Reduced Extracellular Matrix Stiffness Prompts SH-SY5Y Cell Softening and Actin Turnover To Selectively Increase Aβ(1–42) Endocytosis. *ACS Chemical Neuroscience, 10* (3), 1284-1293. doi:10.1021/acschemneuro.8b00366

Li, Y., & Kumacheva, E. (2018). Hydrogel microenvironments for cancer spheroid growth and drug screening. *Science Advances, 4* (4), eaas8998. doi:10.1126/sciadv.aas8998

López-Marcial, G. R., Zeng, A. Y., Osuna, C., Dennis, J., García, J. M., & O'Connell, G. D. (2018). Agarose-Based Hydrogels as Suitable Bioprinting Materials for Tissue Engineering. *ACS Biomaterials Science & Engineering, 4* (10), 3610-3616. doi:10.1021/acsbiomaterials.8b00903

Malmqvist, M. (1978). Degradation of agarose gels and solutions by bacterial agarase. *Carbohydrate Research, 62* (2), 337-348. doi:https://doi.org/10.1016/S0008-6215(00)80880-0

Monaco, G., Cholas, R., Salvatore, L., Madaghiele, M., & Sannino, A. (2017). Sterilization of collagen scaffolds designed for peripheral nerve regeneration: Effect on microstructure, degradation and cellular colonization. *Mater Sci Eng C Mater Biol Appl, 71* , 335-344. doi:10.1016/j.msec.2016.10.030

Monteiro, M. V., Gaspar, V. M., Ferreira, L. P., & F., M. J. (2020). Hydrogel 3D in vitro tumor models for screening cell aggregation mediated drug response. *Biomater Sci*

8 (7), 1855-1864. doi:10.1039/c9bm02075f

Napolitano, A. P., Dean, D. M., Man, A. J., Youssef, J., Ho, D. N., Rago, A. P., . . . Morgan, J. R. (2007). Scaffold-free three-dimensional cell culture utilizing micromolded nonadhesive hydrogels. *Biotechniques, 43* (4), 494, 496-500. doi:10.2144/000112591

Nath, S., & Devi, G. R. (2016). Three-dimensional culture systems in cancer research: Focus on tumor spheroid model. *Pharmacol Ther, 163* , 94-108. doi:10.1016/j.pharmthera.2016.03.013

Nguyen-Ngoc, K. V., Cheung, K. J., Brenot, A., Shamir, E. R., Gray, R. S., Hines, W. C., . . . Ewald, A. J. (2012). ECM microenvironment regulates collective migration and local dissemination in normal and malignant mammary epithelium. *Proc Natl Acad Sci U S A, 109* (39), E2595-2604. doi:10.1073/pnas.1212834109

Oza, M. D., Prasad, K., & Siddhanta, A. K. (2012). One-pot synthesis of fluorescent polysaccharides: adenine grafted agarose and carrageenan. *Carbohydrate Research, 357* , 23-31. doi:https://doi.org/10.1016/j.carres.2012.05.016

Petibois, C., Gouspillou, G., Wehbe, K., Delage, J. P., & Déléris, G. (2006). Analysis of type I and IV collagens by FT-IR spectroscopy and imaging for a molecular investigation of skeletal muscle connective tissue. *Anal Bioanal Chem, 386* (7-8), 1961-1966. doi:10.1007/s00216-006-0828-0

Ranamukhaarachchi, S. K., Modi, R. N., Han, A., Velez, D. O., Kumar, A., Engler, A. J., & Fraley, S. I. (2019). Macromolecular crowding tunes 3D collagen architecture and cell morphogenesis. *Biomaterials Science, 7* (2), 618-633. doi:10.1039/c8bm01188e

Shin, S., Ikram, M., Subhan, F., Kang, H. Y., Lim, Y., Lee, R., . . . Yoon, S. (2016). Alginate–marine collagen–agarose composite hydrogels as matrices for biomimetic 3D cell spheroid formation. *RSC Advances, 6* (52), 46952-46965. doi:10.1039/C6RA01937D

Singh, A., Brito, I., & Lammerding, J. (2018). Beyond Tissue Stiffness and Bioadhesivity: Advanced Biomaterials to Model Tumor Microenvironments and Drug Resistance.*Trends in Cancer, 4* (4), 281-291. doi:10.1016/j.trecan.2018.01.008

Tang, Y., Liu, J., & Chen, Y. (2016). Agarose multi-wells for tumour spheroid formation and anti-cancer drug test. *Microelectronic Engineering, 158* , 41-45. doi:https://doi.org/10.1016/j.mee.2016.03.009

Tasdemir, N., Bossart, E. A., Li, Z., & Zhu, L. (2018). Comprehensive Phenotypic Characterization of Human Invasive Lobular Carcinoma Cell Lines in 2D and 3D Cultures.*78* (21), 6209-6222. doi:10.1158/0008-5472.can-18-1416

Teruki, N., Kimiko, M., & Yasuhiko, T. (2020). Three-Dimensional Culture System of Cancer Cells Combined with Biomaterials for Drug Screening. *Cancers, 12* (10), 2754 (2751-2724).

doi:https://doi.org/10.3390/cancers12102754

Terzi, A., Storelli, E., Bettini, S., Sibillano, T., Altamura, D., Salvatore, L., . . . Giannini, C. (2018). Effects of processing on structural, mechanical and biological properties of collagen-based substrates for regenerative medicine.*Scientific Reports, 8* (1), 1429. doi:10.1038/s41598-018-19786-0

Tian, Z., Liu, W., & Li, G. (2016). The microstructure and stability of collagen hydrogel cross-linked by glutaraldehyde. *Polymer Degradation and Stability, 130* , 264-270. doi:https://doi.org/10.1016/j.polymdegradstab.2016.06.015

Tibbitt, M. W., & Anseth, K. S. (2009). Hydrogels as extracellular matrix mimics for 3D cell culture.*Biotechnology and Bioengineering, 103* (4), 655-663. doi:10.1002/bit.22361

Trappmann, B., Gautrot, J. E., Connelly, J. T., Strange, D. G. T., Li, Y., Oyen, M. L., . . . Huck, W. T. S. (2012). Extracellular-matrix tethering regulates stem-cell fate.*Nature Materials, 11* (7), 642-649. doi:10.1038/nmat3339

Ulrich, T. A., Jain, A., Tanner, K., MacKay, J. L., & Kumar, S. (2010). Probing cellular mechanobiology in three-dimensional culture with collagen-agarose matrices.*Biomaterials, 31* (7), 1875-1884. doi:10.1016/j.biomaterials.2009.10.047

Vergara, D., Simeone, P., Franck, J., Trerotola, M., Giudetti, A., Capobianco, L., . . . Maffia, M. (2016). Translating epithelial mesenchymal transition markers into the clinic: Novel insights from proteomics. *EuPA Open Proteomics, 10* , 31-41. doi:https://doi.org/10.1016/j.euprot.2016.01.003

Wang, Y., Gong, T., Zhang, Z. R., & Fu, Y. (2017). Matrix Stiffness Differentially Regulates Cellular Uptake Behavior of Nanoparticles in Two Breast Cancer Cell Lines. *ACS Appl Mater Interfaces, 9* (31), 25915-25928. doi:10.1021/acsami.7b08751

Wong, S. H. M., Fang, C. M., Chuah, L. H., Leong, C. O., & Ngai, S. C. (2018). E-cadherin: Its dysregulation in carcinogenesis and clinical implications. *Crit Rev Oncol Hematol, 121* , 11-22. doi:10.1016/j.critrevonc.2017.11.010